Halogen Chemistry

Deutsche Ausgabe: DOI: 10.1002/ange.201510641
Internationale Ausgabe: DOI: 10.1002/anie.201510641

Evidence for Interfacial Halogen Bonding

Wesley B. Swords, Sarah J. C. Simon, Fraser G. L. Parlane, Rebecca K. Dean, Cameron W. Kellett, Ke Hu, Gerald J. Meyer, and Curtis P. Berlinguette**

Abstract: *A homologous series of donor–π–acceptor dyes was synthesized, differing only in the identity of the halogen substituents about the triphenylamine (TPA; donor) portion of each molecule. Each* ***Dye-X*** *(X = F, Cl, Br, and I) was immobilized on a TiO_2 surface to investigate how the halogen substituents affect the reaction between the light-induced charge-separated state, $TiO_2(e^-)$/**Dye-X**$^+$, with iodide in solution. Transient absorption spectroscopy showed progressively faster reactivity towards nucleophilic iodide with more polarizable halogen substituents:* ***Dye-F*** *<* ***Dye-Cl*** *<* ***Dye-Br*** *<* ***Dye-I****. Given that all other structural and electronic properties for the series are held at parity, with the exception of an increasingly larger electropositive σ-hole on the heavier halogens, the differences in dye regeneration kinetics for* ***Dye-Cl****,* ***Dye-Br****, and* ***Dye-I*** *are ascribed to the extent of halogen bonding with the nucleophilic solution species.*

A halogen bond is an attractive non-covalent interaction between a halogen and a nucleophilic species.[1–6] Halogen bonding has been characterized in fluid solution and in solid state materials with applications in crystal engineering, anion sensing, self-assembly, biotechnology, and catalysis.[7–22] Reported herein is kinetic evidence indicating that halogen bonding also occurs at the solid–liquid interface. This finding was enabled by systematic characterization of a homologous series of donor–π–acceptor dyes, varying only in the identity of two halogen atoms, at titanium dioxide acetonitrile interfaces (Scheme 1). Light-induced interfacial electron transfer experiments revealed enhanced photoreactivity when larger, more polarizable halogens were employed. This result offers compelling evidence that halogen bonding assists the regeneration of the photo-oxidized dyes, which is supported by computational data. The observation that halogen bonding can occur at solid–liquid interfaces and has a measurable effect on charge-transfer behavior, suggests that it can be exploited in applications, including solar energy conversion schemes.

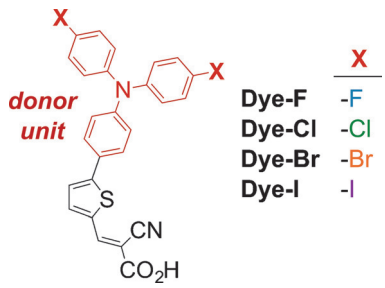

Scheme 1. Molecular structure of the **Dye-X** (X = halogen) series.

The ability of a halogen atom in an organohalide compound to act as a Lewis acid arises from an electropositive "σ-hole" in the halogen np_z orbital, surrounded by a belt of negative charge from the filled ns and $np_{x,y}$ orbitals.[23,24] An important feature of the σ-hole is that it increases with the polarizability and principle quantum number (n) of the halogen.[3,23–25] In the case of organo-iodide compounds in solution, the free energy change that accompanies halogen bonding can be upwards of 10 kcal mol^{-1}, but is completely absent for the corresponding fluoride compounds.[10–13] In contrast, other intermolecular forces, such as those between ions and dipoles, increase with the electronegativity of the halogen atom. However, the small size of the fluorine atom can lead to some exceptions. Hence, systematic studies of a series of donor–π–acceptor dyes, where the halogens are positioned on atoms far from the surface binding group, may provide new insights into non-covalent interactions at interfaces and a means by which dipolar and halogen bonding interactions can be distinguished.

Dyes were synthesized that differed only in the two halogen atoms positioned *para* with respect to the nitrogen atom of the TPA donor moiety (Scheme 1). These dye molecules were anchored to mesoporous TiO_2 thin films commonly used in dye-sensitized solar cells, with typical surface coverages of 4×10^{-8} mol cm^{-2}.[26] Importantly, immobilized dyes may eliminate the interference of some intermolecular reactions between the dye molecules that would otherwise occur in solution. Immobilization also offers control over the dipole orientation of the dye, allowing the halogen bond donor access to the nucleophilic species in solution.[27] Additionally, the ability of TiO_2 to quantitatively accept electrons from the dye excited states provides the opportunity to photo-initiate interfacial electron transfer and iodide oxidation reactions that may be influenced by surface dipoles or secondary bonding interactions.[28–33] Nanosecond transient absorption and computational studies of the **Dye-X** series outlined herein reveal evidence for halogen bonding interactions between iodide and the immobilized photo-

[*] W. B. Swords, Dr. K. Hu, Prof. G. J. Meyer
Department of Chemistry,
The University of North Carolina at Chapel Hill
Murray Hall 2202B, Chapel Hill, NC 27599-3290 (USA)
E-mail: gjmeyer@email.unc.edu
S. J. C. Simon, F. G. L. Parlane, Dr. R. K. Dean, C. W. Kellett, Prof. C. P. Berlinguette
Departments of Chemistry and Chemical & Biological Engineering,
The University of British Columbia
2036 Main Mall, Vancouver, BC V6T1Z1 (Canada)
E-mail: cberling@chem.ubc.ca

Supporting information for this article can be found under: http://dx.doi.org/10.1002/anie.201510641.

oxidized dyes, $TiO_2(e^-)$/**Dye-X**$^+$, where X is a heavy halogen atom.

DFT modeling of the **Dye-X** and **Dye-X**$^+$ compounds, shown in Figure 1, confirms that a σ-hole is indeed present opposite the covalently bound carbon on the heavier halogen atoms X = Cl, Br, and I (Figure 1).[34] The electropositivity of the σ-hole increases upon oxidation and with halogen polarizability. Note that **Dye-F** shows a negligible σ-hole in the ground and oxidized states, whereas **Dye-I** has a significant positive charge on the poles of each halogen that increases upon oxidation. The σ-hole is opposite to the X–C bond and can therefore accommodate a 180° R-X···nucleophile bond angle, which is expected and is well documented in the solid state literature.[24]

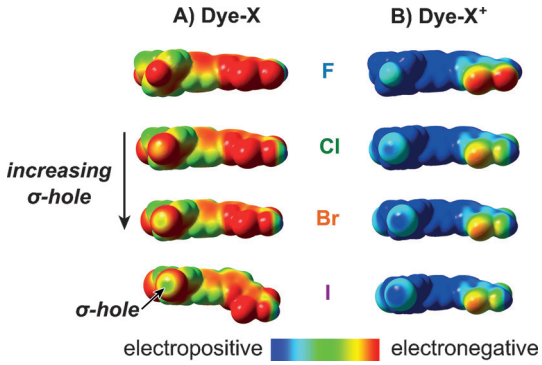

Figure 1. DFT models of the A) neutral and B) oxidized forms of **Dye-X** show the existence of a σ-hole on the pole of the halogen atoms opposite the covalently bound atom for X = Cl, Br, and I. The electrostatic potential was plotted over the total electron density at an absolute isovalue of 0.001.[23,35] Darkest red represents a potential of −8.79 kcal mol^{-1}; darkest blue represents a potential of 54.6 kcal mol^{-1}.

The TiO_2/**Dye-X** materials displayed quasi-reversible TiO_2/**Dye-X**$^{+/0}$ redox chemistry by cyclic voltammetry (Figure 2). The frontier orbitals predicted by DFT analysis, as well as prior research, indicate that the redox chemistry is localized on the TPA donor portion of the molecules; that is, TPA$^{\bullet+}$/TPA^0.[27] The difference in reduction potentials were 50 mV for TiO_2/**Dye-F** and TiO_2/**Dye-Cl**, and merely 15 mV spanning TiO_2/**Dye-Cl**, TiO_2/**Dye-Br**, and TiO_2/**Dye-I** (Table 1). The aforementioned data indicates that the identities of the halogen atoms do not significantly influence the dye electronic structures, thereby enabling interfacial reactivity to be quantified without appreciable differences in the driving force (ΔG^o) for the series. Importantly, the redox couples reside at a more positive potential than the relevant one-electron redox potentials associated with iodide oxidation.

Pulsed light excitation of TiO_2/**Dye-X** in $NaClO_4$ solutions (0.3 M in CH_3CN) resulted in the immediate appearance of the oxidized dye molecule. Such behavior is consistent with rapid excited state injection, $k_{inj} > 10^8$ s^{-1}, known for this class of dye molecules [Eq. (1)].[27] Excited state injection and recombination to the oxidized dyes, $k_{rec} \approx 130$ s^{-1} [Eq. (2)], were insensitive to the presence of the halogen atoms. The

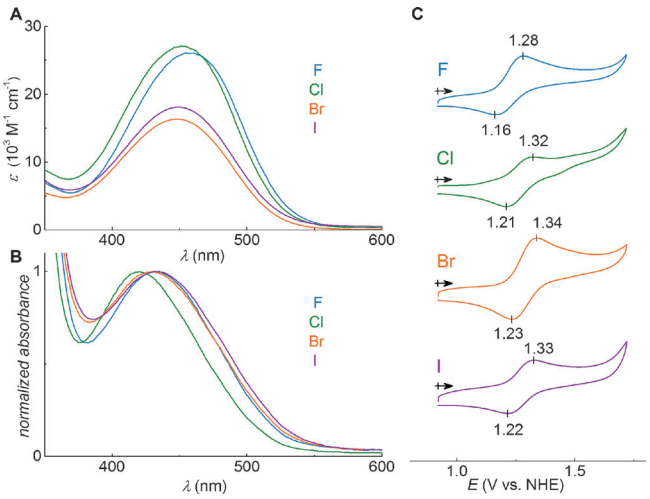

Figure 2. UV/Vis absorption spectra for A) **Dye-X** and B) TiO_2/**Dye-X**. C) Cyclic voltammograms of TiO_2/**Dye-X**. Data is summarized in Table 1.

Table 1: Optical, redox, and dye regeneration data for **Dye-X**.[a]

Compound	λ_{abs} [nm]	E^o [V][b]	k_{reg} [$\times 10^8$ M^{-1} s^{-1}][c]
Dye-F	432	1.22	4.7
Dye-Cl	420	1.27	8.8
Dye-Br	429	1.28	10.9
Dye-I	432	1.27	13.5

[a] Data measured in CH_3CN solutions at room temperature.
[b] TiO_2/**Dye-X** measured in $NaClO_4$ (0.3 M) electrolyte at 100 mV s^{-1} and externally referenced to $Fc^{+/0}$ (+0.64 V vs. NHE).
[c] Corresponds to the slopes of the linear fits in Figure 3 B.

similar recombination rates are likely because of the modest structural and thermodynamic changes (ca. 50 meV) associated with inclusion of the halogen atoms.

$$TiO_2/\textbf{Dye-X} \rightarrow TiO_2(e^-)/\textbf{Dye-X}^+ \quad (1)$$

$$TiO_2(e^-)/\textbf{Dye-X}^+ \rightarrow TiO_2/\textbf{Dye-X} \quad (2)$$

The regeneration of $TiO_2(e^-)$/**Dye-X**$^+$ by I^- [Eq. (3)] was investigated at five different iodide concentrations from 0.5 to 10.0 mM. Representative data for the TiO_2/**Dye-X** series, quantified under low irradiance to ensure pseudo first-order conditions, is shown in Figure 3. This comparison is particularly useful as the free energy change for the reaction is the same within experimental error, and the σ-hole for TiO_2/**Dye-I** was significantly larger. The observed absorption transients were non-exponential in all cases and were well-described by the Kohlrausch–Williams–Watts function [Eq. (4)], as described by other groups.[36–38] The first moment of the function was taken as an observed "average" rate constant, k_{obs} [Eq. (5)]. Here, β is inversely related to a Levy distribution of rate constants and was fixed to 0.69 over all the kinetic data.[39,40]

$$TiO_2(e^-)/\textbf{Dye-X}^+ + 2\,I^- \rightarrow TiO_2(e^-)/\textbf{Dye-X} + I_2^{\bullet-} \quad (3)$$

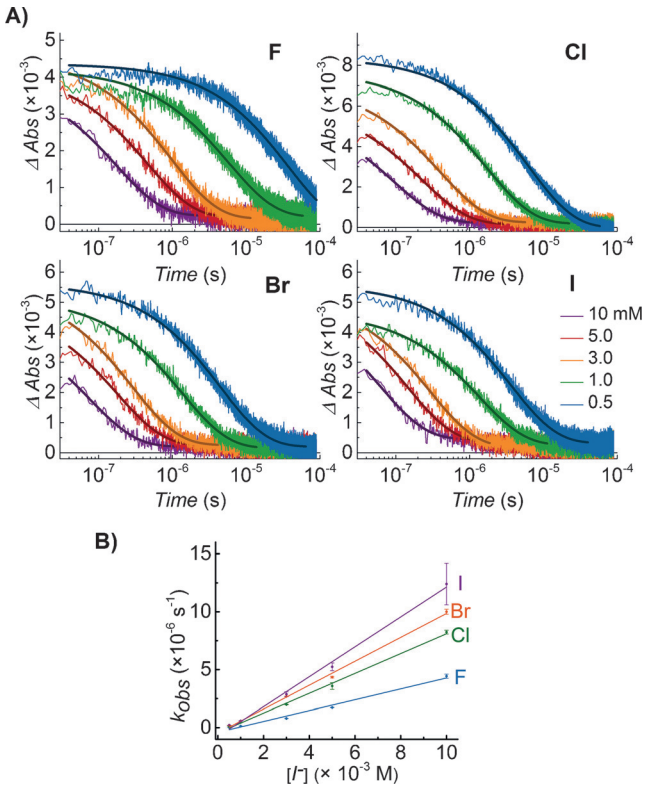

Figure 3. A) Single wavelength kinetic data of $TiO_2(e^-)$/**Dye-X**$^+$ and I^- at iodide concentrations of 0.5–10 mM in $NaClO_4$ (0.3 M in CH_3CN) solutions. Dyes were excited at 532 nm and probed near the peak of the oxidized spectrum: 610, 620, 630, and 630 nm for X = F–I, respectively. B) Overlaid plots of k_{obs} obtained from kinetic fitting of the single wavelength kinetic data. The regeneration rate constants for the reaction are listed in Table 1.

$$A(t) = A_0 e^{-(kt)^{\beta}} \quad (4)$$

$$k_{obs} = \frac{k\beta}{\Gamma(\frac{1}{\beta})} \quad (5)$$

The k_{obs} values increased linearly with iodide concentration and the slopes abstracted from this data yielded the second-order regeneration rate constants (k_{reg}; Figure 3). The values for k_{reg} span about a factor of three and follow the trend TiO_2/**Dye-I** > TiO_2/**Dye-Br** > TiO_2/**Dye-Cl** > TiO_2/**Dye-F** (Table 1). Note that iodide oxidation is known to occur by two distinct mechanisms, one that is first-order and the other second-order in iodide concentration. With the exception of the first-order pathway for $TiO_2(e^-)$/**Dye-F**$^+$, both mechanisms are thermodynamically favored at these interfaces, E^o $(I^{\bullet}/I^-) = 1.23$ V and E^o $(2\,I^-/I_2^{\bullet-}) = 0.93$ vs. NHE.[41] While there is no direct experimental evidence for a pathway that is second-order in iodide, it would be more likely when halogen bonding brings two iodide ions within proximity of the TPA donor group in the dye molecules. Indeed, previous workers have invoked composite mechanisms to rationalize the rapid kinetics of the intermolecular reaction where ion-pairing between the oxidant and iodide precedes electron transfer.[42,43] In this regard, halogen bonding provides an attractive alternative for iodide association at these interfaces that does not require the presence of a cationic dye. High concentrations of iodide are important for solar energy conversion near the maximum power point condition, and specific interactions with the oxidized TPA may help promote the second-order pathway. We note that regeneration studies were not carried out with Br^- and Cl^-, as was done with I^-, because of thermodynamic considerations.

The regeneration rate constants for the $TiO_2(e^-)$/**Dye-X**$^+$ series were progressively larger as the size of the halogen increased, data that cannot be rationalized based on the thermodynamic driving force of the reaction. For example, iodide oxidation was approximately 1.5 times faster for $TiO_2(e^-)$/**Dye-I**$^+$ than for $TiO_2(e^-)$/**Dye-Cl**$^+$, even though the free energy change was the same. Likewise, if the kinetics were solely driven by thermodynamics, $TiO_2(e^-)$/**Dye-Br**$^+$ would have the largest regeneration rate constant; contrary to what was measured.

Attempts to identify halogen bonding with the TiO_2/**Dye-X** compounds through anion recognition and halide titration experiments, similar to those widely used in solution studies, proved inconclusive. The absorption spectrum of TiO_2/**Dye-F** and TiO_2/**Dye-I** showed a similar blue shift upon addition of 5 mM tetrabutylammonium salts of Cl^-, Br^-, and I^- (Supporting Information, Figure S1). These shifts can be ascribed to non-halogen bonding interactions of the added halides near the TPA unit. There was no reason to suspect that these interactions were responsible for the observed trend in regeneration rates, as **Dye-F** and **Dye-I** displayed the same anion-induced absorption shift, yet with vastly different k_{reg} values (Table 1). It is unsurprising that evidence for halogen bonding was absent in these titration studies, as prior research in homogeneous solutions indicates that the halogen must be attached to an exceptionally electron deficient ring to observe anion recognition spectroscopically.[2] Anion recognition experiments with the oxidized dyes were unsuccessful because of dye desorption from the surface.

DFT models were generated for the proposed **Dye-X**···I^- interactions by optimizing each structure with an iodide ion positioned 4.5 Å from the pole of one of the constituent halogen atoms (Supporting Information, Figure S5). The interaction energy (ΔE_{int}) of each system was obtained by taking the difference between the optimized single-point energy, corrected for basis set superposition error (BSSE) using the counterpoise method, and the energy of a non-interacting system where iodide was positioned 12 Å from the dye. The value of ΔE_{int} was found to be 2.65 kcal mol^{-1} lower for **Dye-I** than for **Dye-F**, with a concomitant 0.59 Å contraction in internuclear distances (Table 2). The **Dye-X**···I^- distances were calculated to be shorter than predicted based on van der Waals radii for **Dye-Br** and **Dye-I**, while the values for **Dye-F** and **Dye-Cl** were beyond the predicted van der Waals distances. This data, which tracks with the σ-hole character for the dyes, is illustrated by the intermolecular potential energy plotted as a function of distance (Figure 4).

Natural bond orbital (NBO) analysis describes the principal **Dye-X**···I^- interaction as a donation of a lone pair on iodide into the empty C-X σ* orbital. The stabilization

Table 2: Calculated intermolecular interaction metrics.

Compound	$d_{(X\cdots I)}$ [Å][a]	van der Waals [Å][b]	ΔE_{int} [kcal mol^{-1}][c]	E^2 [kcal mol^{-1}][d]
Dye-F	4.28	3.53	−0.07	0.06
Dye-Cl	3.86	3.81	−0.40	1.30
Dye-Br	3.68	3.91	−1.52	4.04
Dye-I	3.69	4.04	−2.72	6.76
Dye-I$^+$	3.61	4.04	−4.06	8.53

[a] Optimized internuclear distance between the halogen atom and iodide ion. [b] Total van der Waals for X and iodide interaction. [c] BSSE corrected interaction energy. [d] Stabilization energy from donation of the I$^-$ lone pair into the C–X anti-bond, determined by NBO analysis.

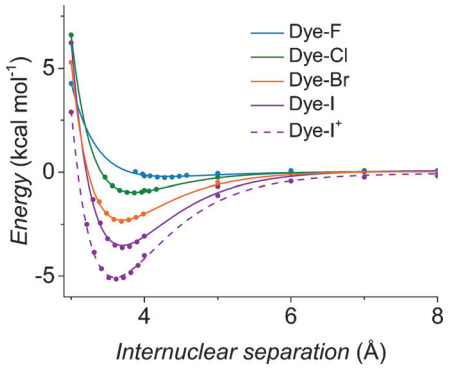

Figure 4. Change in the potential energy as a function of the halogen–iodide distance. The energy measured at a separation of 11 Å is taken as $E = 0$ kcal mol^{-1}.

energy (E^2) of this interaction increased significantly for the heavier halogen substituents (Table 2; Supporting Information, Table S1). Similar analyses performed on structures optimized with different iodide starting positions (Supporting Information; Figures S6 and S7, Tables S2 and S3) did not reveal significant periodic trends.

To confirm that this description of the **Dye-X**···I$^-$ interaction was still valid in the oxidized state, we carried out the same computational analysis with **Dye-I**$^+$. The **Dye-I**$^+$···I$^-$ interaction shortened by 0.08 Å and ΔE_{int} decreased by 1.34 kcal mol^{-1} relative to the values determined for neutral **Dye-I** (Table 2). NBO analysis reveals a 1.77 kcal mol^{-1} increase in E^2 for donation of an I$^-$ lone pair into the empty C-I σ* orbital, but otherwise does not suggest any significant changes in the nature of this interaction. This result indicates that the decrease in ΔE_{int} upon oxidation was exclusively because of an increase in the strength of the halogen bond. These collective computational results indicate that the extent of halogen bonding does affect the strength of the intermolecular interaction between the dye and iodide.

Previous computational and experimental studies have shown that halogen bonding interactions are more significant as the size of the halogen atoms increases (I > Br > Cl), while the magnitude of the molecular dipole is expected to show the opposite trend. Herein, this behavior was exploited to study non-covalent interactions and test whether halogen bonding can occur at sensitized semiconductor–liquid interfaces. Nanosecond kinetic studies coupled with DFT analysis provide compelling evidence that indicates halogen bonding is operative. The regeneration rate constants follow the trend I > Br > Cl > F, which cannot be rationalized with thermodynamic considerations. While other non-covalent interactions were certainly at play, given the homologous structures of the series and similar electronic properties, we ascribe these observed trends to the increased propensity of the more polarizable halogen substituents to participate in halogen bonding. This finding, which is supported by computational data, suggests that halogen bonding may be used to control the distribution of ions at an illuminated interface. This behavior may be exploited for solar energy conversion and heterogeneous catalysis.

Acknowledgements

The authors declare no competing financial interests. UNC authors acknowledge support by a grant from the Division of Chemical Sciences, Office of Basic Energy Sciences, Office of Energy Research, U.S. Department of Energy (DE-SC0013461) and by the National Science Foundation Graduate Research Fellowship Program under grant no. DGE-1144081. (W.B.S). UBC authors are grateful to the Canadian Natural Science and Engineering Research Council, the Canadian Foundation for Innovation, CIFAR, and Canada Research Chairs for support.

Keywords: dyes · halogen bonding · inorganic chemistry · semiconductor interfaces · reaction kinetics

How to cite: *Angew. Chem. Int. Ed.* **2016**, *55*, 5956–5960
Angew. Chem. **2016**, *128*, 6060–6064

[1] P. Metrangolo, G. Resnati, *Chem. Eur. J.* **2001**, *7*, 2511–2519.
[2] M. Erdélyi, *Chem. Soc. Rev.* **2012**, *41*, 3547–3557.
[3] P. Metrangolo, H. Neukirch, T. Pilati, G. Resnati, *Acc. Chem. Res.* **2005**, *38*, 386–395.
[4] O. Hassel, *Science* **1970**, *170*, 497–502.
[5] P. Metrangolo, G. Resnati, T. Pilati, S. Biella, in *Halogen Bonding*, Springer, Berlin, Heidelberg, **2008**, pp. 105–136.
[6] S. L. Price, A. J. Stone, J. Lucas, R. S. Rowland, A. E. Thornley, *J. Am. Chem. Soc.* **1994**, *116*, 4910–4918.
[7] W. T. Pennington, T. W. Hanks, H. D. Arman, in *Halogen Bonding*, Springer, Berlin, Heidelberg, **2008**, pp. 65–104.
[8] M. G. Sarwar, B. Dragisic, S. Sagoo, M. S. Taylor, *Angew. Chem. Int. Ed.* **2010**, *49*, 1674–1677; *Angew. Chem.* **2010**, *122*, 1718–1721.
[9] P. Metrangolo, G. Resnati, *Science* **2008**, *321*, 918–919.
[10] T. M. Beale, M. G. Chudzinski, M. G. Sarwar, M. S. Taylor, *Chem. Soc. Rev.* **2013**, *42*, 1667–1680.
[11] A. Caballero, F. Zapata, N. G. White, P. J. Costa, V. Félix, P. D. Beer, *Angew. Chem. Int. Ed.* **2012**, *51*, 1876–1880; *Angew. Chem.* **2012**, *124*, 1912–1916.
[12] M. J. Langton, S. W. Robinson, I. Marques, V. Félix, P. D. Beer, *Nat. Chem.* **2014**, *6*, 1039–1043.
[13] S. W. Robinson, C. L. Mustoe, N. G. White, A. Brown, A. L. Thompson, P. Kennepohl, P. D. Beer, *J. Am. Chem. Soc.* **2015**, *137*, 499–507.
[14] S. H. Jungbauer, S. M. Huber, *J. Am. Chem. Soc.* **2015**, *137*, 12110–12120.

[15] A. Vanderkooy, M. S. Taylor, *J. Am. Chem. Soc.* **2015**, *137*, 5080 – 5086.
[16] J. Lieffrig, O. Jeannin, M. Fourmigué, *J. Am. Chem. Soc.* **2013**, *135*, 6200 – 6210.
[17] L. Meazza, J. A. Foster, K. Fucke, P. Metrangolo, G. Resnati, J. W. Steed, *Nat. Chem.* **2012**, *5*, 42 – 47.
[18] Q.-N. Zheng, X.-H. Liu, T. Chen, H.-J. Yan, T. Cook, D. Wang, P. J. Stang, L.-J. Wan, *J. Am. Chem. Soc.* **2015**, *137*, 6128 – 6131.
[19] S. V. Rosokha, M. K. Vinakos, *Phys. Chem. Chem. Phys.* **2014**, *16*, 1809 – 1813.
[20] T. Shirman, T. Arad, M. E. van der Boom, *Angew. Chem. Int. Ed.* **2010**, *49*, 926 – 929; *Angew. Chem.* **2010**, *122*, 938 – 941.
[21] M. Boterashvili, T. Shirman, S. R. Cohen, G. Evmenenko, P. Dutta, P. Milko, G. Leitus, M. Lahav, M. E. van der Boom, *Chem. Commun.* **2013**, *49*, 3531 – 3533.
[22] T. Shirman, R. Kaminker, D. Freeman, M. E. van der Boom, *ACS Nano* **2011**, *5*, 6553 – 6563.
[23] T. Clark, M. Hennemann, J. S. Murray, P. Politzer, *J. Mol. Model.* **2007**, *13*, 291 – 296.
[24] P. Politzer, P. Lane, M. C. Concha, Y. Ma, J. S. Murray, *J. Mol. Model.* **2007**, *13*, 305 – 311.
[25] P. Politzer, J. S. Murray, T. Clark, *Phys. Chem. Chem. Phys.* **2010**, *12*, 7748 – 7757.
[26] S. Ardo, G. J. Meyer, *Chem. Soc. Rev.* **2009**, *38*, 115 – 164.
[27] K. C. D. Robson, K. Hu, G. J. Meyer, C. P. Berlinguette, *J. Am. Chem. Soc.* **2013**, *135*, 1961 – 1971.
[28] A. Reynal, A. Forneli, E. Martinez-Ferrero, A. Sánchez-Díaz, A. Vidal-Ferran, B. C. O'Regan, E. Palomares, *J. Am. Chem. Soc.* **2008**, *130*, 13558 – 13567.
[29] F. Liu, G. J. Meyer, *J. Am. Chem. Soc.* **2005**, *127*, 824 – 825.
[30] J. K. McCusker, *Acc. Chem. Res.* **2003**, *36*, 876 – 887.
[31] B. C. O'Regan, K. Walley, M. Juozapavicius, A. Anderson, F. Matar, T. Ghaddar, S. M. Zakeeruddin, C. Klein, J. R. Durrant, *J. Am. Chem. Soc.* **2009**, *131*, 3541 – 3548.
[32] M. Planells, L. Pellejà, J. N. Clifford, M. Pastore, F. De Angelis, N. López, S. R. Marder, E. Palomares, *Energy Environ. Sci.* **2011**, *4*, 1820 – 1829.
[33] A. Hagfeldt, G. Boschloo, L. Sun, L. Kloo, H. Pettersson, *Chem. Rev.* **2010**, *110*, 6595 – 6663.
[34] A.-C. C. Carlsson, J. Gräfenstein, A. Budnjo, J. L. Laurila, J. Bergquist, A. Karim, R. Kleinmaier, U. Brath, M. Erdélyi, *J. Am. Chem. Soc.* **2012**, *134*, 5706 – 5715.
[35] R. F. W. Bader, M. T. Carroll, J. R. Cheeseman, C. Chang, *J. Am. Chem. Soc.* **1987**, *109*, 7968 – 7979.
[36] A. Y. Anderson, P. R. F. Barnes, J. R. Durrant, B. C. O'Regan, *J. Phys. Chem. C* **2011**, *115*, 2439 – 2447.
[37] Y. Bai, J. Zhang, D. Zhou, Y. Wang, M. Zhang, P. Wang, *J. Am. Chem. Soc.* **2011**, *133*, 11442 – 11445.
[38] T. Daeneke, A. J. Mozer, Y. Uemura, S. Makuta, M. Fekete, Y. Tachibana, N. Koumura, U. Bach, L. Spiccia, *J. Am. Chem. Soc.* **2012**, *134*, 16925 – 16928.
[39] C. P. Lindsey, G. D. Patterson, *J. Chem. Phys.* **1980**, *73*, 3348 – 3357.
[40] G. Williams, D. C. Watts, *Trans. Faraday Soc.* **1970**, *66*, 80 – 85.
[41] J. G. Rowley, B. H. Farnum, S. Ardo, G. J. Meyer, *J. Phys. Chem. Lett.* **2010**, *1*, 3132 – 3140.
[42] D. M. Stanbury, W. K. Wilmarth, S. Khalaf, H. N. Po, J. E. Byrd, *Inorg. Chem.* **1980**, *19*, 2715 – 2722.
[43] G. Nord, *Comments Inorg. Chem.* **1992**, *13*, 221 – 239.

Received: November 17, 2015
Revised: February 19, 2016
Published online: April 8, 2016

